Integration of ERS-1 PRI Imagery and Digital Terrain Models for the Assessment of Flooded Areas

A. Giacomelli, M. Mancini and R. Rosso DIIAR - Politecnico di Milano, P.zza L. da Vinci 32, 20133, Milano ITALIA
andreag crs4.it
http://www.crs4.it/~andreag

Abstract

Spaceborne radar sensors, with their exclusive cloud penetration capacity, have an interesting potential in the monitoring of flood events. A procedure for the identification of inundated areas from ERS-1 PRI imagery is proposed and demonstrated for the flood which occurred in Northern Italy in November 1994. The extremely high sensitivity of the radar signal to surface roughness allows to easily identify from the SAR data the fields reached by the flooding water as low-backscatter areas. However, the availability of single-band, single-polarization data, such as in the case of ERS-1, may lead to uncertainties in the identification of the flooding condition of vegetated sites or, in general, where the height of the flooding water is lower than the elements determining the roughness of the imaged scene. The application of multitemporal analysis is certainly an aid in the solution of this problem, but since at C band the penetration capacity of vegetation is know to be rather low, it may not be completely able to solve the ambiguities in the image. The integration of the remotely sensed imagery with a digital terrain model and the application of a simple conceptual drainage scheme may represent an additional technique to overcome this limitation, with the advantage of requiring a single image, and very littl e processing of the radar data The use of a geographic information system greatly simplifies the implementation of the procedure (which can be developed using simple terrain analysis functions) and draws the attention on the need for more accurate digital terrain models.

Keywords: flood monitoring, GIS, SAR, integration, DTMs

1. Introduction

Regional-scale monitoring has become a primary tool in natural resource management, especially in situations of emergency, when the priority is given to the timeliness of an overall picture of the situation, rather than to its accuracy. Satellite remote sensing has a great potential in this field, with its ability to investigate very wide areas in a very short time and with a high temporal frequency, with subsequent overpasses, on the same site, up to a few days one from the other for Earth observation satellites.

In the case of floodplain monitoring, the importance of remote sensing lies not only in the possibility of being an aid to land planning and to studying the impact of a flood event in populated areas. Research both in ecology and in biology may benefit from a more accurate knowledge of floodplain inundation patterns in tropical forest regions, since it would be possible to define more accurately the rates of production and decomposition of organic matter. Similarly, an improvement in the assessment of natural wetlands would improve the estimates on the production of atmospheric methane, which is an important greenhouse gas (Hess *et al.* 1990). The application of remote sensing in the field of flooded area assessment has been studied for some time, employing both passive (Rango and Salomonson 1974, Blasco *et al.* 1992) and active (Hess *et al.* 1990) sensors, obtaining interesting results over areas characterized by very different conditions in morphology, climate and land use. Generally, the objective of such research has been limited to inferring information on the extension reached by a flooding; in some cases, however, it is possible to derive from the remotely sensed data also additional information, such as the profile of an in-transit flood wave in a valley (Brakenridge *et al.* 1994). Techniques for the assessment of the damage caused by inundations directly from satellite remotely sensed data have also been proposed, albeit limited to specific land uses. For instance, Yamagata and Akiyama (1988) were able to use Landsat 5 Thematic Mapper imagery to estimate paddy rice damage and the corresponding decrease in rice yield caused by flooding, by relating these factors to the turbidity of the flood water. Always based on the detection of suspended sediment from optical data, Mertes (1996) showed that it is possible to discriminate the source of flood water, which may originate either from the river network, or from the surge of the water table, thus allowing a new insight in the dynamics of flooding.

Passive sensors are capable of detecting flooded areas also several days after the water has retreated from the flooded fields, either by recognition of the sediment which is left on the area, or by monitoring of vegetation stress (Rango and Salomonson 1974); thus, they can be considered useful tools in the case of an *a posteriori* assessment of the effects of an inundation However, the spectral bands used by these instruments do not allow to penetrate cloud cover, which is a constant presence during a flooding event. For this reason they cannot provide satisfactory results in the case of real time (or quasi-real time) monitoring or -at any rate- if the cloud cover over the imaged scene is not limited. An active sensor can easily overcome the obstacle represented by cloud cover, but it may encounter some problems in the assessment of the flooding condition of vegetated sites. In fact, with the availability of a single-band, single-date data set. it is impossible to separate, in the return signal, the contribution of soil surface backscattering from the contribution of vegetation scattering.

Several paths may be followed to improve this situation. For instance, it is possible to use *multi-sensor* techniques, combining SAR data with information acquired by other platforms -typically LANDSAT or SPOT- shortly after the flood event (Wang *et al.* 1995). Employing only remotely sensed data, multi-sensor techniques seem best suited over areas which cannot be easily accessed, or for which there is a lack of other data. However, for the same reason, it is necessary to rely on at least two different sensors, so there is first of all a problem of an effective availability of these data at the right moment, which depends on the orbits of the different satellites. Secondly, there is a problem of actually processing the large amount of data which, originating from different instruments, will require different processing techniques. Following a different approach, the radar imagery may be merged with data which are not retrieved at the moment of the event, derived from different sources (including other remotely sensed imagery). In this case, the amount of information which must be collected at the occurrence of the event is minimized, and for this reason the computational load in the ``operative'' phase is reduced. In this framework we may consider the *multi-temporal* approach: the effects of the event can be related to the *change detection* between two or more SAR images, acquired before and after the flooding, assuming that the variations in the radar response due to other causes -such as changes in land cover or viewing geometry- can be neglected. In principle, multi-temporal analysis should represent the simplest approach to inundated area assessment, being the co-registration of the images the only strictly required processing. However, it is should be verified whether the investigated phenomenon (the presence of water, in this case) can be detected effectively on all the possible land cover types that may be encountered in the scene. The European Space Agency is providing a world-wide web-based service (referred to as ``Earth Images on Special Events''), dedicated to the diffusion of imagery of ``special'' events which are well identified by the ERS-1 satellite, such as oil spills, large fires, volcanic eruptions and floods. In the latter case, multi-temporal analysis is used to highlight the extension of the flooded areas. Another possibility of combining ``static'' data with the imagery acquired during the flooding event is to integrate the information obtained from a simple preprocessing of the radar data with digital terrain models (DTMs). This possibility has been explored in this study, by means of algorithms developed using terrain analysis functions available in many geographical information system (GIS) packages. Compared to the other two solutions, this approach minimizes the necessary computational resources and the data requirements in terms of remotely sensed imagery to be retrieved at the moment of the flooding, because most of the information may be processed off-line, being the SAR imagery the only data to be acquired during the event.

2. RESPONSE OF FLOODED AREAS TO THE RADAR SIGNAL

The identification of a completely flooded field, as well as of the river network and of the water bodies, is quite simple: their backscattering is in fact very low, due to the practically specular reflection of the incident signal (Figure 1A). If a water body is large enough, the action of wind may lead to the formation of ripples -and eventually waves- on the water surface, determining an increase in the backscattering coefficient, due to the increased roughness of the target. However, this effect is reasonably neglectable on the majority of flooded sites. Vegetated areas yield a more complex radar response (Figure 1C): the incident wave is partly scattered directly from the top layer of the canopy (leaves, branches), and partly transmitted to the lower layer (trunks or stems) and to the soil. This part of the signal is subject to additional scattering, and is then returned to the sensor, after a second passage through the upper layer. The backscattering coefficient measured from a flooded vegetated area may then be higher with respect to the same area in dry conditions, with an increment which may exceed 6 dB (Ormsby *et al.* 1985). This is due to the fact that the layer of water underlying the vegetation reflects completely the incident energy, making it wholly available for further scattering from the leaves and the branches, whilst normally it would have been scattered by the soil. The magnitude of this effect depends on sensor frequency, since it will be possible to penetrate only obstacles which have characteristic dimensions significantly smaller than the corresponding wavelength. At L band ($\lambda \simeq$ 20 cm) satisfactory results have been achieved in the identification of inundated vegetated areas (Ormsby *et al.* 1985, Hess *et al.* 1990), while with only C band available ($\lambda \simeq$ 5 cm), and with a single-date data set -as in the case of ERS-1 - we may expect only part of the actually flooded areas to be identified; the increase in σ° will be much smaller, since the largest fraction of the signal will be scattered by the uppermost layer of the foliage. The importance of this effect is understandable, considering the strong presence of high-trunk vegetation (typically poplars) in the high-water beds along the rivers in the area examined in the following case study. Urban sites will yield in any case a very high backscattering coefficient, because of the *corner reflector* effect generated by the buildings. Such a radar response does not allow the presence of surface water to be detected very clearly (Figure 1B). It should also be noted that, during or immediately after a flooding, we expect all non-flooded targets to have in any case a higher water content. Soil and biomass water content will be very high in all parts of the scene, and there may be a presence of water droplets on leaves and branches, determining an increase in the dielectric constant of a target. This fact is responsible for an additional variation to the backscattering behaviour, thus additionally complicating the interpretation of the scene, if only a single channel of information is available, as in the case of ERS-1.

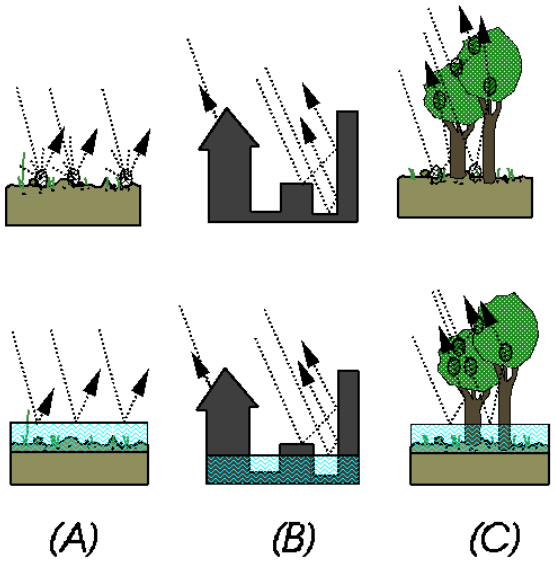

Figure 1: Effect of a layer of standing water on the radar signal. The short dotted segments and the hatched circles indicate the presence of scattering, while the arrowheads indicate the direction taken by the prevailing outgoing signal

3. CASE STUDY: PIEMONTE, NOVEMBER 1994

The case study analyzed in this dissertation is focused on the November 1994 flooding in Northern Italy, which has been one of the most catastrophic events occurred in Italy in the last forty years. In the case study presented the lower part of the Tanaro catchment (in the Region of Piemonte) has been considered, between the towns of Felizzano and Alessandria. For this site a detailed (1:10000) thematic cartography was available, showing the extension of the inundated areas. The ground truth available at the moment of the analysis does not cover all the region selected for this study, but only two thirds of it: the lower right and lower left quadrants are missing. Figure 2 shows the part of the PRI frame corresponding to the area selected for the analysis, covering 960x1680 pixels (i.e. 12x21 Km²). This window has been georeferenced on the cartographic data set, with a rectification error of around 10 metres. The river Tanaro and the river Bormida clearly stand out, the latter flowing on the right side of the image. The city of Alessandria is also visible, represented by the higher intensity pixels between the two rivers. The main elements of the transportation network can also be observed: the Torino-Piacenza highway, represented by the dark line running in the East-West direction, and the Voltri-Santhià highway (runnning from North to South), with their junction just outside Alessandria.

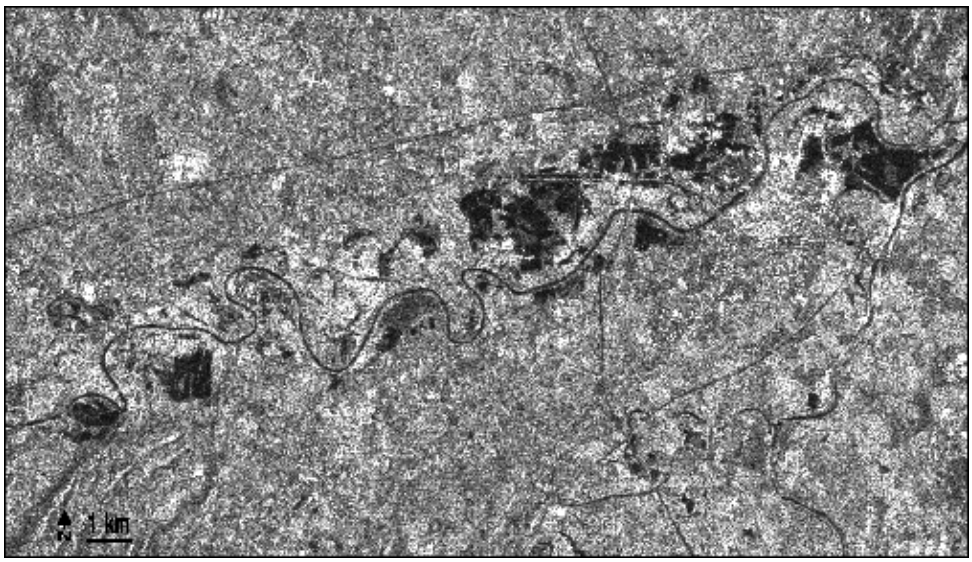

Figure 2: ERS-1 PRI SAR image of the Tanaro river between Felizzano and Alessandria (on the right) during the 1994 flooding. The image has been acquired on November 9.

Coming to the classification of the inundated areas, it can be seen that even a first qualitative analysis gives a fair idea of the extension of the flooding, identified by the lower intensity areas. In some cases the tonal variations allow to identify interesting features such as boundaries between agricultural fields or traces of ancient drainage patterns. However, a comparison with ground truth indicates that a consistent part of the inundated area yields a strong response in the radar image. This suggests that the backscattering from the soil may be masked by the contribution of the canopy -as described in Section 2- and points out the need for a procedure in order to overcome the resulting uncertainties in the interpretation. Backscattering values are stored in the PRI products as 2-byte integer digital numbers, from which full-precision values of σ° can be derived by application of a calibration coefficient and of a column-dependent correction factor (Laur, 1993). This correction yields a variation of about 1 dB from near range to far range, but in the proposed application it has been neglected, because a high radiometric precision is not considered necessary: in fact, the SAR data are used only to derive a first estimate for the extension of the flooded area, and the σ° values are not employed in any calculation. This avoids the need for the use of floating point operations, thus allowing to reduce substantially the computation time in each phase of the processing. A digital elevation model (DEM) of the area is also available, with a resolution of 7.5''x10'' (latitude by longitude), which projected is approximately 230x220 m². This resolution appears to be quite low if compared to that of the radar data; however, this was the only DEM available at the moment of the analysis.

THE ``DRAINAGE-ON-DTM'' ALGORITHM

From the previous sections it may be gathered that the only flooded areas which can be detected without ambiguity from PRI data are those in which the height of the water completely submerges surface roughness, i.e. characterized by a very low backscattering. The possibility of deriving reliable conclusions on the areas of intermediate intensity appears questionable, due to the fact that the contributions of the different scattering layers cannot be separated. Analyzing the image, it appears that the river network and the more visibly flooded fields are characterized by digital number values lower than 160-200. If all pixels with a grey level above this treshold are discarded, we obtain the result indicated in Figure 3. This includes also clusters of very few pixels, which do not actually correspond to ``smooth'' areas, but to the effect of speckle, and which must be discarded. This is justified remembering that a physically significant value for σ° may be computed only for a distributed target. Laur (1993) suggests using a sample of at least 400 pixels, but in fact it is observed that even clusters with a much smaller size correspond to actual features on the ground. In this case a threshold of 50 pixels has been taken, generating a ``base layer'' which can be considered as a first-approximation estimate for the inundated area (Figure 4). This is a fairly raw filtering technique, but its approximation is accepted, since it does not lead to the final result, but only to the starting point for the following algorithm. The parts of the image outlined with this operation correspond to less than 10% of the actually flooded area. This percentage may vary depending on the canopy height distribution in the flooded site and on the intensity of the flooding event, but it cannot be considered in any case a very satisfactory estimate.

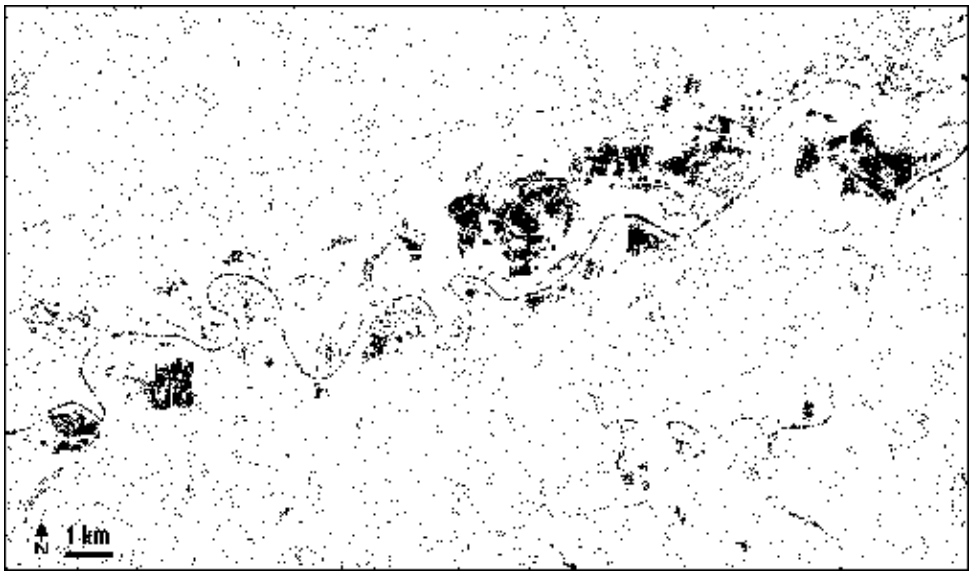

Figure 3: Parts of the image with DN < 160

Figure 3: Parts of the image with DN < 160.

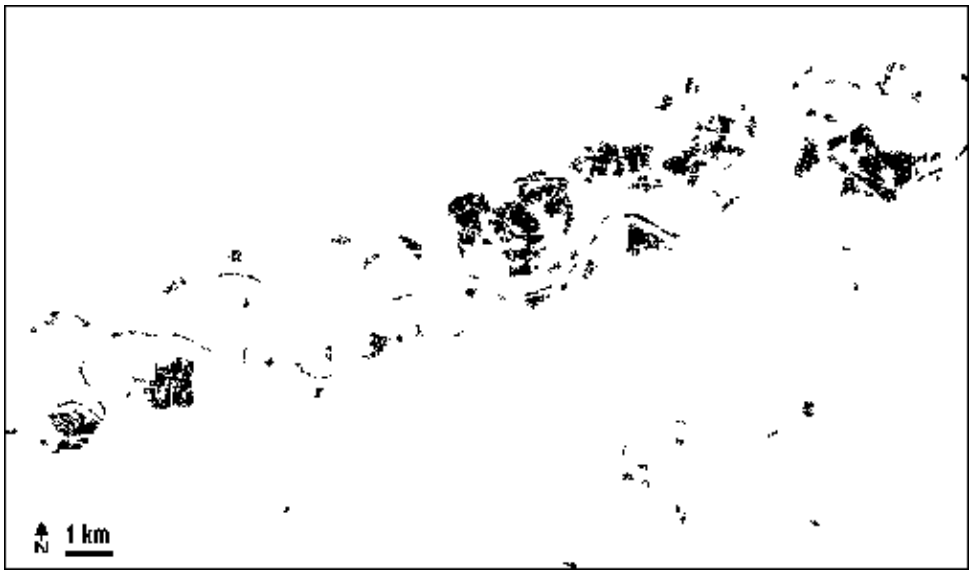

Figure 4: Result of the removal of the smaller clusters.

At this point we assume that the water occupying the areas highlighted by the SAR may flow on the natural drainage network, a process which can be easily simulated employing a least-cost algorithm (Khawaja 1993), which is a standard tool in many GIS packages. This algorithm takes as input a matrix, whose values represent the ``cost'' of passing through a cell, and computes the least-cost path from a given starting point on the matrix itself. If the DEM is used as a cost matrix, and the areas now identified as sets of starting points, additional areas in which the presence of water can be expected are obtained, as demonstrated by Figure 5. A cell in the DEM may be crossed by flow from more than one drainage path, each one deriving from a different starting point. The output of the algorithm is represented by a raster layer bearing for each cell the number of crossings which have occurred. From here on, this procedure will be referred to as *DOD* (``drainage-on-DTM'').

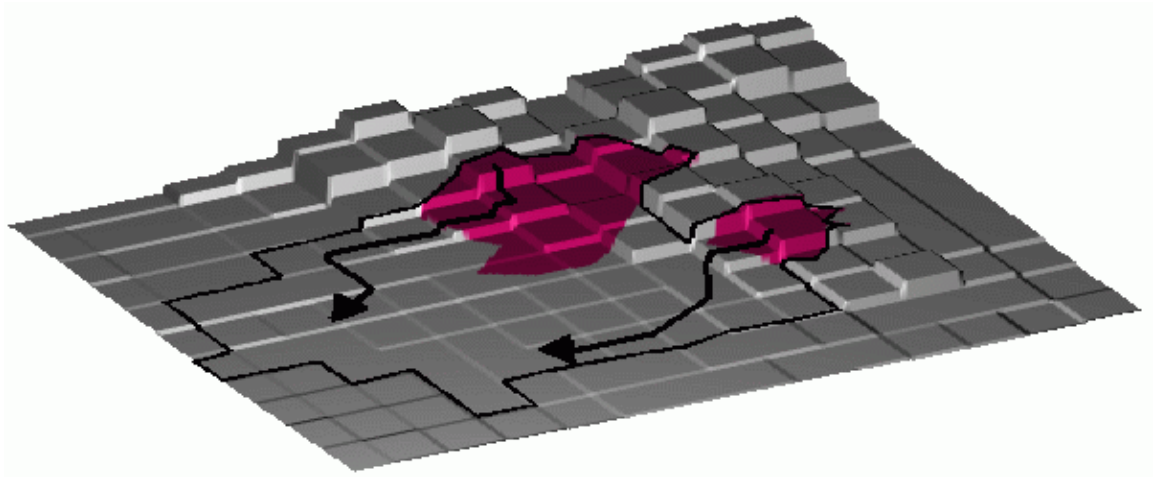

Figure 5: The DOD procedure: using the low-backscatter patches as starting points for the least cost algorithm, additional areas where the presence of water can be expected are identified.

From a conceptual point of view, the *DOD* algorithm, albeit ``physically based'', does not reflect the actual dynamics of the flooding process: a more appropriate treatment would imply the use of sophisticated bidimensional unsteady flow hydraulic models, with strong problems in the parameterization and in the definition of their boundary conditions. However, the scope of the proposed procedure is not to simulate the inundation, but to produce a map indicating the presence of water, over a large area, possibly with a low computational effort. From this point of view, we believe that the proposed procedure may be of some interest, considering its simplicity within a GIS environment and its ``slim'' data requirements.

APPLICATION OF THE *DOD* TO THE ALESSANDRIA SITE

Figure 6 shows the result of the application of the *DOD* algorithm to the base layer. A consistent improvement can be observed, even though the area of the inundated zone remains underestimated: compared to the base layer (in Figure 4, corresponding to approximately 10% of the flooded area) the DOD output covers 50 to 60% of the flooded area, the actual value depending on the fine-tuning of some of the algorithm parameters (Giacomelli, 1997). However, in terms of uniformity of the estimate, results are satisfactory: in fact, the largest of the non-recognized areas measures less than 2 km².

The need for a DEM at a higher resolution, and with a greater accuracy, is clear from the result shown in the central part of Figure 6 where the algorithm has located a flooded area which is surely non-existent, between the limits of the area inundated by the two rivers, Tanaro and Bormida. This issue becomes even more important due to the fact that the analysis is performed in a floodplain area, so even small errors in the DEM may have a strong influence on the result.

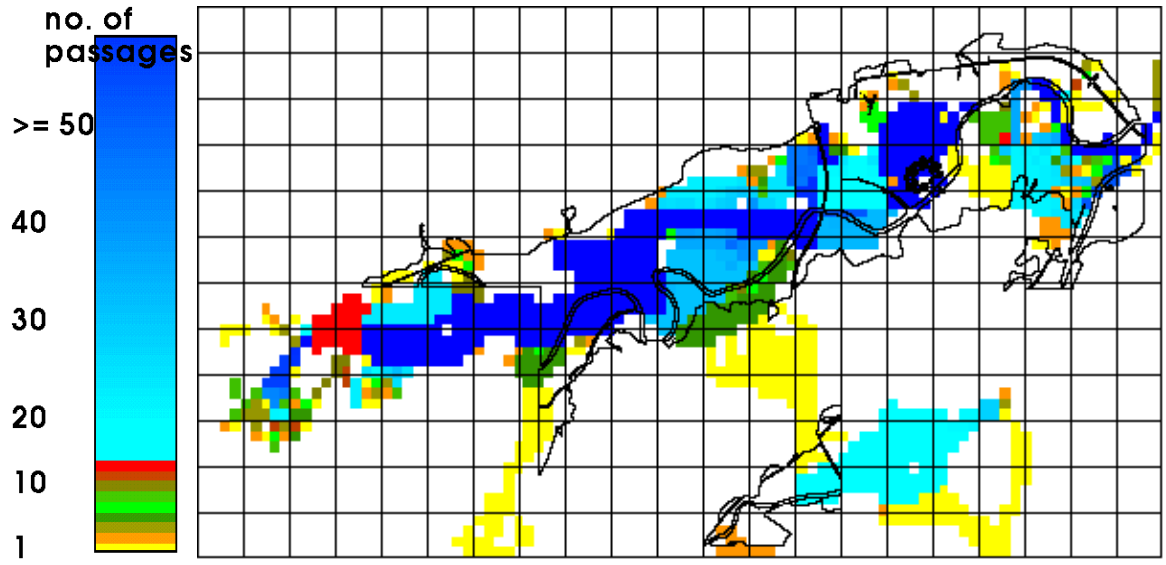

Figure 6: An example of the result obtained by the DOD algorithm; The color code corresponds to the number of simulated flow crossings in a cell. The reference grid has a 1-Km spacing.

This result shows also that there will be some inconsistencies, if a ``spurious'' cluster -i.e. a low intensity spot which does not correspond to a flooded area on the ground- is included in the base layer. In fact, the spurious cluster will generate an overestimation error in the output, marking as potentially flooded a drainage path which is actually dry, at least for the part which is not included in the drainage patterns of other clusters. The spurious clusters may indeed correspond to low-return targets, but, considering that the SAR data has undergone a rather simple radiometric processing, their presence may typically be due to unwanted speckle in the image. Some attempts have been made to refine the definition of the base layer, in order to reduce the possibility of such errors. In addition to applying the *DOD* procedure to the *RAW* data, the least-cost algorithm has been run on an image filtered with a 7x7 pixel moving average, and on an image processed with a local statistics Sigma filter (Lee 1983). Table 1 provides a comparison of the performance of the algorithm using these three definitions of the base layer. Three indices are used to evaluate the performance: the total processing time and the two parameters *A'* and *A''*, defined as:

$$A' = 100 \cdot \frac{A_{detected} \cap A_{flooded}}{A_{flooded}}$$

$$A'' = 100 \cdot \frac{A_{detected} \cap A_{dry}}{A_{dry}}$$

A' represents the accuracy of the estimate, in terms of percentage of correctly identified flooded area, while *A''* represents the ``overestimation'' error, i.e. the percentage of non-flooded area which has been classified as potentially flooded by the least-cost algorithm. Note that the processing time does not include the georeferencing of the imagery.

base layer type	preprocessing time	intermediate time	final time	tot time	results *A'*	*A''*
RAW	0'00''	0'45''	4'51''	6'16''	56%	3.5%
AVERAGE	0'15''	0'22''	1'56''	2'33''	47%	1.43%
LEE	6'59''	0'22''	2'11''	9'32''	46%	1.39%

Table 1: Performance of the drainage algorithm obtained using three different criteria for the definition of the base layer.

The differences between the *AVERAGE* and *LEE* outputs are minimal, suggesting that -for the scope of the drainage algorithm- a sophisticated filtering of the SAR data is not required. In fact, a complex speckle reduction procedure would indeed allow to reduce the presence of spurious clusters in the base layer but, at the same time, it would determine the removal of patches which may clearly be classified as water. As a consequence, the overestimation error, *A''*, is more than halved in the case of the filtered base layers, but also *A'* decreases, with a loss of nearly 10% in the estimate of the flooded area. An alternative solution could be to adopt the method yielding the highest value for *A'* and to apply a series of *a posteriori* constraints on the results, thus allowing to discriminate the spurious clusters on the most accurate result. For instance, it is possible to discard all cells characterized by a very low number of algorithm crossings, or lying on the drainage path of a cluster which is far from the river network and -thus- has a low probability of belonging the the actually flooded area. The application of advanced SAR filtering techniques is in any case not strictly recommended.

Conclusions

The coupling of SAR PRI data with digital terrain models appears to be a useful approach to integrate the capability of the ERS-1 sensor in the identification of flooded areas, which is otherwise constrained by its limited possibilities of penetrating the vegetation canopy. In this paper, an algorithm of ``drainage on DTM'' has been presented, in order to locate the areas reached by a flooding event moving from an assessment of the completely submerged fields, which may easily be detected by means of radar imagery. In practice, the *DOD* algorithm is used to extrapolate the result of the identification of these sites, thus bypassing the interpretation of the radar signal deriving from parts of the scene where a correct understanding of the backscattering process cannot be easily achieved if a single channel of radar information (i.e. a single band and a single polarization) is available. The

results obtained, in addition to indicating the need for several improvements in the proposed procedure, also suggest some interesting developments in the research.

The availability of a DEM with a higher resolution, and with a higher accuracy, appears as one of the top priorities, due to the fact that in floodplain areas even small errors in the elevation data may determine strong inconsistencies in the estimation of the drainage patterns. In addition, a higher spatial resolution would allow first of all to overcome the constraint represented by difference in resolution between the radar imagery and the elevation data, which otherwise determines a strong degradation in the description of the base layer. Secondly, a DEM at a higher resolution would allow to consider in the analysis the presence of man-made features, such as enbankments or roads. These structures, which in a GIS are represented as vector features, may in fact condition the extension of the inundation. In order to take into account their effect within the drainage algorithm, it is necessary to convert the vector data to raster format and to incorporate them into the ``cost'' matrix, originally represented only by the DEM. Setting aside the criterium to be followed in assigning a ``crossing cost'' to the cells containing a rasterized infrastructure, it can be seen that the discretization of the vector features on a 200 m-side grid (such as the one of the available DEM) appears too raw, while it would be surely more appropriate with a DEM at a higher resolution (for instance, with a 50x50 m² cell size). It has been shown that the application of more advanced speckle reduction filters does not enhance significantly the overall performance of the *DOD* algorithm, with respect to the use of very simple filtering procedures. Thus, the decision of accepting a much longer processing time, in order to achieve a slightly more accurate estimate of the flooded area, is to be related to subjective considerations, and it cannot be taken *a priori*. The choice may rather be evaluated according to the specific situation, even though in general it is suggested to follow the simplest path, thus reducing the requested computational load. Further research is needed to improve the performance of the algorithm. One of the primary issues is the need for a validation on additional sites, followed by the comparison of the *DOD* with other flooded area estimation techniques, based either on the use of remote sensing data, or on the employment of hydraulic models. In the presented tests, the accuracy reached by the *DOD* algorithm is not very high, with the detection of 50 to 60% of the actually flooded area. Although this may appear a poor performance, the result of the processing of bi-dimensional data should not be assessed only on a global numeric index. The capability of representing the spatial pattern of the inundated area is in fact quite satisfactory: the flooded areas not detected by the least-cost algorithm are not very extended compared to the total, and -generally- they are also encircled by *DOD*-derived patches. The relative simplicity of the adopted methodology -added to the fact of georeferencing being the only strictly necessary processing step on the remotely sensed data- suggests the possibility of performing flood mapping over wide areas, with a high spatial resolution and with a low computing time. Under this light it is also possible to understand the role that the *DOD* algorithm takes with respect to the bi-dimensional hydraulic models employed in the simulation of a flooding event. Even though these models are capable of providing a more correct description of the inundation, they are also characterized by a more critical parameterization. For this reason, it cannot be stated *a priori* that these models insure the possibility of yielding a more accurate final result.

From a conceptual point of view, the extension of the *DOD* algorithm to the complete ERS-1 frames -in order to generate region-wide flooding maps- is immediate, and it does not require any modification of the processing algorithm, provided that additional care is taken in the generation of the base layer. Since the full-size radar scene comprises a much higher target heterogeneity, surely a greater number of spurious starting clusters will tend to be included in the starting point set. This is due to the presence of low-backscattering areas, such as the shadowed parts of the relief, or of small water bodies, isolated from the river network, such as artificial lakes or quarries. This problem may be dealt with by excluding from the analysis the parts of the radar image where flooding is not expected, on the basis of constraints implemented by terrain analysis. For instance, it would be possible to exclude the pixels which lay above a certain altitude (absolute, or relative to the river), and the areas characterized by a high local slope, or whose distance from the river network is above a given value. The water bodies which are not connected to the river network are normally indicated the more detailed topographic maps, so they may easily be identified and excluded from the radar imagery, once it has been georeferenced.

Acknowledgement
This work has been supported by the Gruppo Nazionale per la Difesa dalle Catastrofi Idrogeologiche grant 95.00273.PF42, and by the EEC grant EV5V-CT94-0446. The authors have equally contributed to this work.

References

Blasco F., M. F. Bellan and M. U. Chaudury, 1992
Estimating the Extent of Floods in Bangladesh Using SPOT data. *Remote Sensing of Environment*, **39**, pp. 167-178.

Brakenridge G. R., J. C. Knox, E. D. Paylor and F. J. Magilligan, 1994
Radar remote sensing aids study of the Great Flood of 1993. *EOS Transactions*, EOS Transactions, American Geophysical Union, **75** (45), pp. 521, 526-527.

ESA-ESRIN
Earth Images on Special Events (URL)

Giacomelli, A., 1997
The integration of synthetic aperture radar remote sensing in the analysis of surface hydrologic processes: soil moisture estimation and flooded area identification. Ph.D. Thesis. Milano, January 1997.

Hess L. L., J. M. Melack and D. S. Simonett, 1990.
Radar detection of flooding beneath the forest canopy: a review. *Int. Journ. Rem. Sens.*, **11** (7), pp. 1313-1325.

Khawaja K., 1993.
GRASS 4.1 Reference Manual. USA Army C.E.R.L.

Laur. H, 1993.
Derivation of σ^{o} from ERS-1 PRI data. ESRIN, Frascati, Italy.

Lee J. S., 1983.
A simple speckle smoothing algorithm for synthetic aperture radar images. *IEEE Trans. Syst., Man, Cybernetics,* **13** (1), 85-89.

Mertes L. A. K., 1996.
Patterns of inundation hydrology for large rivers derived from optical remote sensing data. Proceedings of the *Progress in Electromagnetic Research Symposium*. Innsbruck (Austria), July 1996.

Ormsby J. P., B. J. Blanchard and A. J. Blanchard, 1985.
Detection of lowland flooding using active microwave systems, *Photogrammetric Engineering and Remote Sensing*, **51**, pp. 317-328.

Rango A. and V. V. Salomonson, 1974.
Regional Flood Mapping from Space, *Water Resour. Res.*, **10** (3), pp. 473-484.

Wang Y., B. N. Koopmans and C. Pohl, 1995.
The 1995 flood in The Netherlands monitored from space - a multi-sensor approach, *Int. Journ. Rem. Sens.*, **16** (15), pp. 2735-2739.

Yamagata Y. and T. Akiyama, 1988.
Flood damage analysis using multitemporal Landsat Thematic Mapper data, *Int. Journ. Rem. Sens.*, **9** (3), pp. 503-514.